



HAL
open science

Electrotunable band gaps of one- and two-dimensional photonic crystal structures based on silicon and liquid crystals

J. Arriaga, L. Dobrzynski, Bahram Djafari-Rouhani

► **To cite this version:**

J. Arriaga, L. Dobrzynski, Bahram Djafari-Rouhani. Electrotunable band gaps of one- and two-dimensional photonic crystal structures based on silicon and liquid crystals. *Journal of Applied Physics*, 2008, 104, pp.063108-1-7. 10.1063/1.2975832 . hal-00357332

HAL Id: hal-00357332

<https://hal.science/hal-00357332>

Submitted on 25 May 2022

HAL is a multi-disciplinary open access archive for the deposit and dissemination of scientific research documents, whether they are published or not. The documents may come from teaching and research institutions in France or abroad, or from public or private research centers.

L'archive ouverte pluridisciplinaire **HAL**, est destinée au dépôt et à la diffusion de documents scientifiques de niveau recherche, publiés ou non, émanant des établissements d'enseignement et de recherche français ou étrangers, des laboratoires publics ou privés.

Electrotunable band gaps of one- and two-dimensional photonic crystal structures based on silicon and liquid crystals

Cite as: J. Appl. Phys. **104**, 063108 (2008); <https://doi.org/10.1063/1.2975832>

Submitted: 01 April 2008 • Accepted: 01 July 2008 • Published Online: 23 September 2008

J. Arriaga, L. Dobrzynski and B. Djafari-Rouhani



View Online



Export Citation

ARTICLES YOU MAY BE INTERESTED IN

Announcement: Focus Issue on “Bipedal Locomotion: From Robots to Humans”

Chaos: An Interdisciplinary Journal of Nonlinear Science **18**, 030202 (2008); <https://doi.org/10.1063/1.2975825>

Fabrication of zinc oxide nanorods based heterojunction devices using simple and economic chemical solution method

Applied Physics Letters **93**, 083124 (2008); <https://doi.org/10.1063/1.2975829>

Phase transformations during rapid heating of Al/Ni multilayer foils

Applied Physics Letters **93**, 081903 (2008); <https://doi.org/10.1063/1.2975830>

Lock-in Amplifiers
up to 600 MHz



Zurich
Instruments



Electrotunable band gaps of one- and two-dimensional photonic crystal structures based on silicon and liquid crystals

J. Arriaga,^{1,a)} L. Dobrzynski,² and B. Djafari-Rouhani²

¹*Instituto de Física, Ciudad Universitaria, 18 Sur y San Claudio, Edificio 14-B, 72570 Puebla, Mexico*

²*Institut d'Electronique, de Microélectronique et de Nanotechnologie, UMR CNRS 8520, UFR de Physique, Université des Sciences et Technologies de Lille, 59655 Villeneuve d'Ascq Cédex, France*

(Received 1 April 2008; accepted 1 July 2008; published online 23 September 2008)

One- and two-dimensional photonic crystals based on silicon with infiltrated liquid crystals are investigated in this paper. We show that the photonic band gap can be continuously tuned changing the orientation of the director of the liquid crystal. For the one-dimensional case, we considered arbitrary direction of propagation of the electromagnetic waves, and we show that it is possible to tune the photonic band gap by an adequate orientation of the liquid crystal. For the two-dimensional case and propagation in the plane of periodicity, we show that there exists no complete photonic band gap in the system for both polarizations. We consider two different configurations, square array of solid Si cylinders in liquid crystal background and a triangular array of liquid crystal cylinders surrounded by Si. We show that for the triangular array it is possible to tune the photonic band gap only for the transversal electric modes. We used the plane wave expansion method to solve the Maxwell equations for anisotropic systems. © 2008 American Institute of Physics.

[DOI: [10.1063/1.2975832](https://doi.org/10.1063/1.2975832)]

I. INTRODUCTION

In the last decade photonic crystals (PCs) have attracted a great deal of attention from the research community due to their ability to control the propagation of light in solid materials.¹⁻³ Using this property, several applications and devices have been proposed. For many applications, tunability of photonic band structure through electro-optical effects would be desirable. A promising approach is the combination of semiconductor PCs with liquid crystals (LCs), which allows a tuning of the photonic band gap.⁴⁻¹¹ The characteristic optical anisotropy of LCs due to the molecule configuration and alignment allows one to easily modify their refractive index n and then the optical properties of the entire PC. The infiltration of LCs has been done in opal structures,^{2,3,5} macroporous silicon,^{4,12} one-dimensional (1D), two-dimensional (2D), and three-dimensional PCs.^{6-10,13-15} However, both in the 1D and 2D cases, only particular orientations for the director of the LC have been considered.

In this paper we study theoretically the 1D and 2D PCs with infiltrated LCs. Using the plane wave (PW) expansion, we solve the Maxwell equations for the propagation of electromagnetic (EM) waves in 1D and 2D periodic structures. The PCs consist of a periodic array of two different materials, a dielectric and a LC. For the 1D case we considered arbitrary direction for propagation and for the 2D case we considered square and triangular arrays of circular LC cylinders in a dielectric matrix and propagation in the plane of periodicity. In both 1D and 2D cases we have considered arbitrary direction for the director of the LC. We have selected Si as the dielectric due to the high technological inter-

est existing presently. We show that it is possible to tune the photonic band gap, orientating adequately the LC.

II. THEORETICAL ASPECTS

The general wave equation for an inhomogeneous dielectric structure is given by

$$\nabla \times [\boldsymbol{\epsilon}^{-1}(\mathbf{r}) \nabla \times \mathbf{H}(\mathbf{r})] = \left(\frac{\omega}{c}\right)^2 \mathbf{H}(\mathbf{r}). \quad (1)$$

Of course, the dielectric tensor for a periodic structure made of anisotropic materials is periodic, $\boldsymbol{\epsilon}(\mathbf{r}+\mathbf{R})=\boldsymbol{\epsilon}(\mathbf{r})$, with $\mathbf{R}=n_1\mathbf{a}_1+n_2\mathbf{a}_2+n_3\mathbf{a}_3$ being the lattice vectors generated by the primitive vector \mathbf{a}_i describing the PC. Generally, LCs possess two kinds of dielectric index. One is the ordinary dielectric index ϵ_o and the other is the extraordinary dielectric index ϵ_e . EM waves with the electric field parallel (perpendicular) to the director of the LC have extraordinary (ordinary) dielectric index. For the LC we can choose a coordinate system (principal set of axes) in which the dielectric tensor is diagonal with principal entries ϵ_e parallel and ϵ_o perpendicular to its director \hat{n} , respectively,

$$\boldsymbol{\epsilon}'_{LC} = \begin{pmatrix} \epsilon_o & 0 & 0 \\ 0 & \epsilon_o & 0 \\ 0 & 0 & \epsilon_o \end{pmatrix}. \quad (2)$$

For PCs, we choose the coordinate system fixed with the z -axis along the periodicity for the 1D case and along the axis of the cylinders for the 2D case. The director \hat{n} of the LC can be arbitrarily orientated with respect to these reference frames. The dielectric tensor in the coordinate system of the PC can be computed by

^{a)}Author to whom correspondence should be addressed. Electronic mail: arriaga@sirio.ifuap.buap.mx.

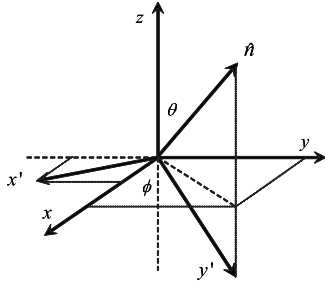


FIG. 1. Coordinate axis (xyz) for the PC and the principal set of axes ($x'y'z'$) of the LC.

$$\epsilon_{LC} = R(\theta, \phi) \epsilon'_{LC} R^T(\theta, \phi), \quad (3)$$

where R is the rotation matrix from the LC principal set of coordinates to the PC coordinate system. The angles θ and ϕ describe the orientation of the director of the LC with respect to the PC coordinate system and this is displayed in Fig. 1. As it can be seen in Fig. 1, θ is the angle between the LC director \hat{n} and the z -axis, and ϕ is the angle between the projection of the LC director on the xy -plane and the x -axis. Once we apply the rotation matrix according to Eq. (3), the elements of the LC dielectric constant tensor in the xyz coordinate system are

$$\epsilon_{xx} = \epsilon_o + (-\epsilon_o + \epsilon_e) \cos^2 \phi \sin^2 \theta,$$

$$\epsilon_{xy} = \epsilon_{yx} = (-\epsilon_o + \epsilon_e) \sin \phi \cos \phi \sin^2 \theta,$$

$$\epsilon_{xz} = \epsilon_{zx} = (-\epsilon_o + \epsilon_e) \cos \phi \cos \theta \sin \theta,$$

$$\epsilon_{yy} = \epsilon_o + (-\epsilon_o + \epsilon_e) \sin^2 \phi \sin^2 \theta,$$

$$\epsilon_{yz} = \epsilon_{zy} = (-\epsilon_o + \epsilon_e) \sin \phi \sin \theta \cos \theta,$$

$$\epsilon_{zz} = \epsilon_o \sin^2 \theta + \epsilon_e \cos^2 \theta. \quad (4)$$

If we consider a PC made of anisotropic materials, the dielectric tensor $\epsilon(\mathbf{r})$ can be expanded in a Fourier series on \mathbf{G} , the reciprocal vectors as

$$\epsilon(\mathbf{r}) = \sum_{\mathbf{G}} \epsilon(\mathbf{G}) \exp(i\mathbf{G} \cdot \mathbf{r}). \quad (5)$$

Using the Bloch theorem we can expand the magnetic field as

$$\mathbf{H}(\mathbf{r}) = \sum_{\mathbf{G}} \sum_{\lambda=1}^2 h_{\lambda}(\mathbf{G}) \hat{\mathbf{e}}_{\lambda}(\mathbf{G}) \exp[i(\mathbf{k} + \mathbf{G}) \cdot \mathbf{r}], \quad (6)$$

where λ labels the two polarizations for any PW in such a way that $\hat{\mathbf{e}}_{\lambda}(\mathbf{G})$, ($\lambda=1,2$), and $\hat{\mathbf{e}}_3(\mathbf{G}) = (\mathbf{k} + \mathbf{G}) / |\mathbf{k} + \mathbf{G}|$ form an orthogonal triad. Inserting Eqs. (5) and (6) into Eq. (1) results in an infinite matrix eigenvalue problem,

$$\sum_{\mathbf{G}'} |\mathbf{k} + \mathbf{G}| \begin{bmatrix} \hat{\mathbf{e}}_2(\mathbf{G}) \cdot \epsilon^{-1}(\mathbf{G}, \mathbf{G}') \cdot \hat{\mathbf{e}}_2(\mathbf{G}') & -\hat{\mathbf{e}}_2(\mathbf{G}) \cdot \epsilon^{-1}(\mathbf{G}, \mathbf{G}') \cdot \hat{\mathbf{e}}_1(\mathbf{G}') \\ -\hat{\mathbf{e}}_1(\mathbf{G}) \cdot \epsilon^{-1}(\mathbf{G}, \mathbf{G}') \cdot \hat{\mathbf{e}}_2(\mathbf{G}') & \hat{\mathbf{e}}_1(\mathbf{G}) \cdot \epsilon^{-1}(\mathbf{G}, \mathbf{G}') \cdot \hat{\mathbf{e}}_1(\mathbf{G}') \end{bmatrix} |\mathbf{k} + \mathbf{G}'| \begin{bmatrix} h_1(\mathbf{G}') \\ h_2(\mathbf{G}') \end{bmatrix} = \left(\frac{\omega}{c}\right)^2 \begin{bmatrix} h_1(\mathbf{G}) \\ h_2(\mathbf{G}) \end{bmatrix}. \quad (7)$$

In this equation, $\epsilon^{-1}(\mathbf{G}, \mathbf{G}') = \epsilon^{-1}(\mathbf{G} - \mathbf{G}')$, where $\epsilon^{-1}(\mathbf{G})$ is the Fourier transform coefficient of $\epsilon^{-1}(\mathbf{r})$. For isotropic PCs, the previous set of equations can be separated into two independent equations satisfied by the two independent polarizations, provided that the direction of propagation of the EM waves is along the direction of periodicity for the 1D PC case and in the plane of periodicity for the 2D case. However, for the anisotropic PCs this decoupling is possible only for particular orientations of the director of LC \hat{n} , and this can be made only if the nondiagonal terms in Eq. (7) are equal to zero, i.e., $\hat{\mathbf{e}}_i(\mathbf{G}) \cdot \epsilon^{-1}(\mathbf{G}, \mathbf{G}') \cdot \hat{\mathbf{e}}_j(\mathbf{G}') = 0$ with $i \neq j$. For arbitrary orientations of the director, we have a system of coupled equations and we must solve it completely. For numerical purposes Eq. (7) is truncated by retaining only a finite number of reciprocal vectors. In the case of PCs with LC components, the dielectric tensor is real and symmetric, and Eq. (7) is likewise a standard real symmetric eigenvalue. The main numerical problem in obtaining the eigenvalues from Eq. (7) is the evaluation of the Fourier coefficients of the inverse dielectric tensor. This can be done as in the case of isotropic materials in two different ways. One can calculate the inverse dielectric tensor in real space and then com-

pute its Fourier coefficients; alternatively, one can calculate the matrix of the Fourier coefficients of the real space tensor and then inverse the matrix to obtain the required Fourier coefficients.¹⁶ This last method was shown to be more efficient for the isotropic tensor and it will be used throughout this paper.

III. 1D PHOTONIC CRYSTALS

The 1D PC studied in this paper consists of alternating layers of anisotropic (LC) and isotropic dielectric media with the z -axis of the PC along the direction of periodicity. The dielectric isotropic media are taken to be Si and the anisotropic media are a LC with two dielectric constants ϵ_e and ϵ_o . For arbitrary orientation of the director \hat{n} , we can choose the orientation of the xyz axes of the PC in such a way that the projection of \hat{n} in the xy plane is along the y -axis, which corresponds to $\phi = \pi/2$. Then the matrix elements different from zero of the dielectric tensor for the anisotropic LC are

$$\epsilon_{LC} = \begin{pmatrix} \epsilon_o & 0 & 0 \\ 0 & \epsilon_o \cos^2 \theta + \epsilon_e \sin^2 \theta & (\epsilon_e - \epsilon_o) \sin \theta \cos \theta \\ 0 & (\epsilon_e - \epsilon_o) \sin \theta \cos \theta & \epsilon_o \sin^2 \theta + \epsilon_e \cos^2 \theta \end{pmatrix}. \quad (8)$$

For on-axis propagation $\hat{\mathbf{e}}_3(\mathbf{G}) = [0, 0, (k+G)/|\mathbf{k}+\mathbf{G}|]$, $\hat{\mathbf{e}}_1 = (1, 0, 0)$, and $\hat{\mathbf{e}}_2 = [0, (k+G)/|\mathbf{k}+\mathbf{G}|, 0]$, where \mathbf{k} and \mathbf{G} are 1D vectors along the z -direction. Then we can write the magnetic field as $\mathbf{H} = H_1 \hat{x} + H_2 \hat{y}$. When we substitute these in Eq. (7), the off-diagonal elements are equal to zero and noticing that the form of $\epsilon^{-1}(\mathbf{G}, \mathbf{G}')$ is similar to Eq. (8), we obtain two independent equations similar to isotropic case,

$$\sum_{\mathbf{G}'} (k+G) \eta_{yy}(\mathbf{G}, \mathbf{G}') (k+G') H_1 = \left(\frac{\omega}{c}\right)^2 H_1, \quad (9)$$

$$\sum_{\mathbf{G}'} |\mathbf{k}+\mathbf{G}| \eta_{xx}(\mathbf{G}, \mathbf{G}') |\mathbf{k}+\mathbf{G}'| H_2 = \left(\frac{\omega}{c}\right)^2 H_2, \quad (10)$$

where $\eta_{ij} = \epsilon_{ij}^{-1}$ is the corresponding block matrix of the inverse matrix dielectric tensor $\epsilon(\mathbf{G}, \mathbf{G}')$. Therefore, we can observe that for arbitrary orientation of the director \hat{n} , we obtain two equations: one equation is independent of the orientation of the director of the LC [Eq. (10)] and one [Eq. (9)] depending on the angle between the director \hat{n} and the direction of periodicity. We can see in Eq. (9) that when the magnetic field is along the x -axis, its corresponding electric field is along the y -axis, and the system of equations uses η_{yy} , which according to Eq. (8) depends on ϵ_o , ϵ_e , and θ . We call this “extraordinary” mode. On the other hand, we see in Eq. (10) that when the magnetic field is along the y -axis, its corresponding electric field is along the x -axis and its associated dielectric constant is ϵ_o [Eq. (10) uses η_{xx}]. We call this “ordinary” mode and it does not depend on the orientation of the director \hat{n} . Of course if $\theta=0$ then both equations are the same and we have the normal solution for an isotropic system with ϵ_o dielectric constant. On the other hand, if the director is perpendicular to the direction of periodicity ($\theta=\pi/2$), the extraordinary mode is governed by ϵ_e as it can be seen in Eq. (8) and the ordinary mode remains unchanged. For conventional 1D PCs with alternating isotropic layers the dielectric constant difference between the two alternating layers is the same for the two components H_1 and H_2 of the magnetic field for propagation along the axis of the system. However, for 1D PCs formed by alternating layers of isotropic and anisotropic materials, the dielectric constant contrast is polarization dependent. The dielectric constant difference for the extraordinary-called and ordinary-called polarizations is $\epsilon(\theta) - \epsilon_b$ and $\epsilon_o - \epsilon_b$, respectively, where ϵ_b is the dielectric constant of the isotropic material (Si in our case). These dielectric constant differences lead to a polarization-dependent band gap. We have done calculations for the 1D PC formed by alternating isotropic Si layers with an $\epsilon_b = 11.9025$ at a wavelength of $1.55 \mu\text{m}$ and anisotropic phenylacetylene LC with $\epsilon_o = 2.5281$ and $\epsilon_e = 4.9284$.⁵ In Fig. 2, we show the band structure calculated for *on-axis* propagation using Eqs. (9) and (10) with the director perpendicular to direction of periodicity z . The band structure displayed in

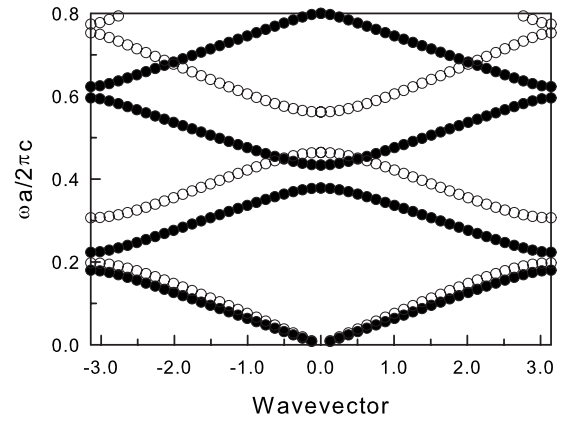


FIG. 2. Band structure for the 1D PC formed by Si/LC periodic array. The width of the LC is $0.8a$. The band structure for ordinary (empty circles) and extraordinary (solid circles) polarizations is presented.

the figure corresponds to a fraction $d_{LC}/d_{Si} = 0.8$ of volume occupied by the LC, and the wavevector k_z is in units of $1/a$, a being the lattice constant. We chose this filling fraction since for this value, and due to the dielectric contrast, the structure possesses a photonic band gap wide enough to stress the effect of the LC orientation. We can clearly observe the different band gaps for both polarizations. The empty circles correspond to the ordinary mode and the solid circles are for the extraordinary modes. Because the ordinary mode does not depend on the orientation of the director of the LC, both results coincide for $\theta=0$. For $\theta \neq 0$ the bands for the extraordinary mode move to low frequencies breaking the degeneracy until they reach the maximum splitting at $\theta=\pi/2$. When the director points along the z -axis, the two lowest complete photonic band gaps are observed from $\Omega = \omega a/2\pi c = 0.197$ to $\Omega = 0.306$ and from $\Omega = 0.4642$ to 0.5618 , respectively. In Fig. 3, we can see the dependence on the gap of the director's orientation \hat{n} of the extraordinary mode, where we plot the two lowest gaps of the structure as a function of the angle θ . The shaded regions correspond to the band gap evolution for the extraordinary mode. The solid lines correspond to the band gaps of the ordinary mode, which is θ independent. As we can see in the figure, we can tune the band gaps of the structure by changing the orientation of the director of the LC. When $\theta=0$ (director along the z -axis) the band structure for both polarizations is the same.

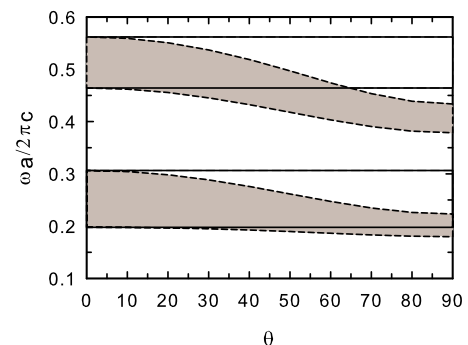


FIG. 3. (Color online) Evolution of the two lowest band gaps as a function of the angle θ of the director \hat{n} of the LC. The solid lines correspond to the gap for the ordinary modes, which are independent of θ . Shaded regions indicate the gaps for the extraordinary modes.

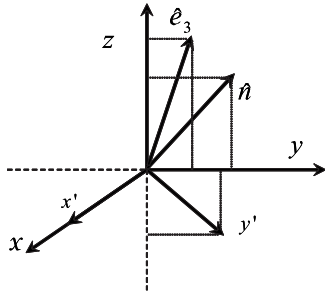


FIG. 4. Coordinate axes for the PC (xyz) and the LC ($x'y'z'$). The direction of propagation of the EM wave is along the \hat{e}_3 direction. The vector \hat{n} and \hat{e}_3 are in the plane yz .

If we increase the angle θ the widths of these two band gaps for the extraordinary mode decrease and move to lower frequencies. This band shift leads to a mismatch in the band gap for both polarizations. The complete photonic band gap for both polarizations is given by the intersection of the shaded areas and the straight lines. We observe that for $\theta > 65^\circ$ the structure still possesses a complete photonic band gap at low frequencies.

For arbitrary direction of propagation, i.e., not along the direction of periodicity, decoupling of Eq. (7) is still possible if both the director \hat{n} and the propagation constant \mathbf{k} are in the same plane. For example, if we take the direction of propagation in the yz plane as is schematically shown in Fig. 4, then $\mathbf{k} = k_y \hat{y} + k_z \hat{z}$. In this case, $\hat{e}_3(\mathbf{G}) = [0, k_y/|\mathbf{k} + \mathbf{G}|, (k_z + G)/|\mathbf{k} + \mathbf{G}|]$, $\hat{e}_1 = (1, 0, 0)$, and $\hat{e}_2 = [0, (k_z + G)/|\mathbf{k} + \mathbf{G}|, -k_y/|\mathbf{k} + \mathbf{G}|]$. Using these vectors in Eq. (7) we obtain a system of equations for the ordinary mode still as Eq. (10), which depends on ϵ_o only. However, the set of equations describing the extraordinary mode is now given by the equation

$$\sum_{\mathbf{G}'} \{ (k_z + G) [\eta_{yy}(k_z + G') - \eta_{yz}k_y] + k_y [-\eta_{zy}(k_z + G') + \eta_{zz}k_y] \} H_1 = \left(\frac{\omega}{c} \right)^2 H_1, \quad (11)$$

which depends on the k_y and k_z components of the propagation constant and includes also the other components of $\eta(\mathbf{G}, \mathbf{G}')$; of course, considering that the propagation of EM waves in arbitrary directions is more realistic in 1D systems. It is worthwhile to observe that the ordinary modes, due to the term $|\mathbf{k} + \mathbf{G}|$ in Eq. (10), also depend on the two components of the propagation constant. We have done calculations for different values of the k_y component of the propagation vector. In Figs. 5(a) and 5(b), we show the band structure with $k_y = 0.5$ (in units of $1/a$) for off-axis propagation for $\theta = 0$ and $\pi/2$, respectively. We can observe from the figures that when we increase the parallel component (k_y) of the propagation vector, there is a variation in the band gap widths of both modes and they move to higher frequencies (compare Fig. 5 and Fig. 2). This behavior can be clearly observed in Figs. 6(a) and 6(b), where we schematically show the evolution of the band gaps as a function of the parallel component of the propagation constant. Figures 6(a) and 6(b) show the evolution of the band gaps when the di-

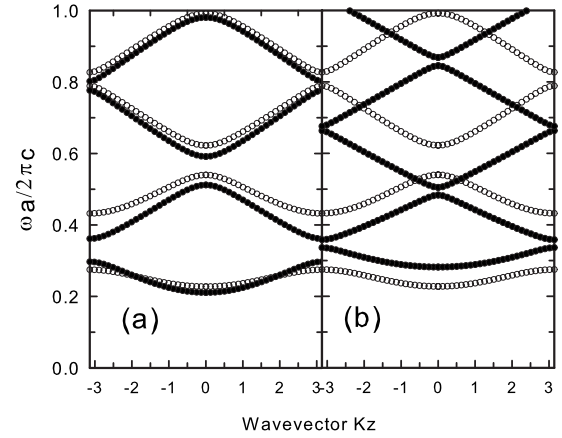


FIG. 5. Band structure for off-axis propagation with $k_y = 0.5$ (in units of $1/a$). (a) $\theta = 0$ and (b) $\theta = \pi/2$. Open circles correspond to the ordinary modes, whereas solid circles correspond to the extraordinary modes.

rector of the LC is parallel and perpendicular to the direction of periodicity, respectively. In Fig. 6(a), for $k_y = 0$ both modes are degenerate and the band gaps correspond to the gaps with $\theta = 0$ of Fig. 3. The dotted and solid lines in Fig. 6 correspond to the gaps for the ordinary modes, whereas the shaded regions correspond to the extraordinary gaps. The complete photonic band gaps for off-axis propagation are given by the intersection between the dotted lines and shaded regions. We observe that when we increase k_y both gaps move to higher frequencies. In the interval studied in this paper $0 \leq k_y \leq 1$ and for the two configurations considered, the width of the lowest band gap for the ordinary modes increases when we increase k_y , whereas the second gap decreases. On the other hand, the band gap widths of the extraordinary modes have a different behavior depending on the orientation of the director \hat{n} . When the director is along the direction of periodicity, the lowest band gap goes to zero at $k_y = 1$. For this configuration and for the interval of frequencies displayed in the figure, the structure possesses two complete photonic band gaps for almost all the values of k_y analyzed here, except for the interval between $0.72 \leq k_y \leq 0.8$, in which we observe

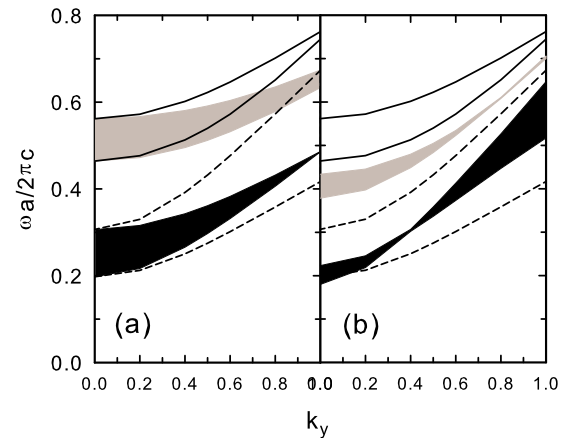


FIG. 6. (Color online) Evolution of the lowest band gaps for the ordinary (solid and dashed lines) and extraordinary (shaded regions) modes as a function of the parallel component k_y of the wavevector. (a) Director \hat{n} parallel to the direction of periodicity. (b) Director \hat{n} perpendicular to the direction of periodicity.

only one gap. From Fig. 6(b) we observe that because the ordinary mode is independent of θ , the widths of these bands are the same as in Fig. 6(a). The only difference between Fig. 6(a) and Fig. 6(b) is the evolution of the extraordinary modes. We observe a different behavior when comparing both figures. The lowest band gap of Fig. 6(b) moves to higher frequencies decreasing its width until it reaches the minimum value around $k_y=0.4$, and from that point it increases reaching its maximum value at $k_y=1$. For this configuration the structure possesses only one complete photonic band gap because the higher bands never intersect. From all these results we observe that the evolution of the band gaps depends not only on the orientation of the director of the LC but also on the direction of propagation of the EM waves.

IV. 2D PHOTONIC CRYSTALS

We have studied as well 2D PCs made of LC cylinders in a square array embedded in a solid silicon matrix. The cylinders run along the z -axis. They are infinitely long and the periodic array is in the xy -plane. If the director of the LC is along the axis of the cylinders (z -axis), then the matrix elements different from zero of the dielectric tensor are

$$\epsilon_{\text{LC}} = \begin{pmatrix} \epsilon_o & 0 & 0 \\ 0 & \epsilon_e & 0 \\ 0 & 0 & \epsilon_e \end{pmatrix}. \quad (12)$$

On the other hand, if the director \hat{n} of the LC is in the plane of periodicity xy , ($\theta=\pi/2$), then the dielectric tensor has the following expression:

$$\epsilon_{\text{LC}} = \begin{pmatrix} \epsilon_o \sin^2 \phi + \epsilon_e \cos^2 \phi & (-\epsilon_o + \epsilon_e) \sin \phi \cos \phi & 0 \\ (-\epsilon_o + \epsilon_e) \sin \phi \cos \phi & \epsilon_o \cos^2 \phi + \epsilon_e \sin^2 \phi & 0 \\ 0 & 0 & \epsilon_o \end{pmatrix}. \quad (13)$$

If we propagate the EM waves along the plane of periodicity, and this is the only case considered in this work, then both the \mathbf{G} vectors and the propagation vector \mathbf{k} are 2D vectors, and for the two configurations mentioned before, we can still separate Eq. (7) into two independent sets of equations for the two independent modes. If we chose $\hat{\mathbf{e}}_1=(0,0,1)$ and taking into account that $\hat{\mathbf{e}}_3(\mathbf{G})=(\mathbf{k}+\mathbf{G})/|\mathbf{k}+\mathbf{G}|$ is in the plane of periodicity, then $\hat{\mathbf{e}}_2=[(k_y+G_y)/|\mathbf{k}+\mathbf{G}|, -(k_x+G_x)/|\mathbf{k}+\mathbf{G}|, 0]$. Because the magnetic field is written as $\mathbf{H}=H_1\hat{\mathbf{e}}_1+H_2\hat{\mathbf{e}}_2$, if we insert the unitary vectors in Eq. (7), the nondiagonal terms are equal to zero and we obtain the following set of uncoupled equations,

$$\begin{aligned} & \sum_{\mathbf{G}'} \{ (k_y + G_y) [\eta_{xx}(\mathbf{G}, \mathbf{G}') (k_y + G'_y) \\ & - \eta_{xy}(\mathbf{G}, \mathbf{G}') (k_x + G'_x)] - (k_x + G_x) [\eta_{yx}(\mathbf{G}, \mathbf{G}') (k_y + G'_y) \\ & - \eta_{yy}(\mathbf{G}, \mathbf{G}') (k_x + G'_x)] \} H_1 = \left(\frac{\omega}{c} \right)^2 H_1, \end{aligned} \quad (14)$$

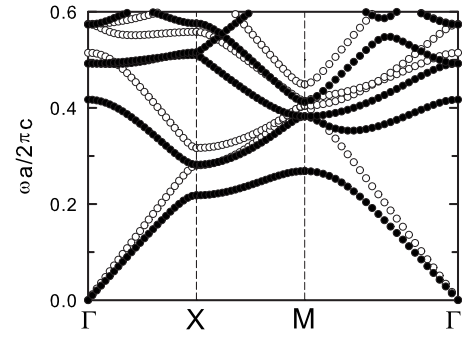


FIG. 7. Band structure for the TE (open circles) and TM (solid circles) modes for a square lattice of solid Si cylinders embedded in a LC matrix. The director \hat{n} is along the axis of the cylinders.

$$\sum_{\mathbf{G}'} |\mathbf{k} + \mathbf{G}'| \eta_{zz}(\mathbf{G}, \mathbf{G}') |\mathbf{k} + \mathbf{G}'| H_2 = \left(\frac{\omega}{c} \right)^2 H_2. \quad (15)$$

In Eq. (14), the magnetic field is along the axis of the cylinders and these modes are called transversal electric (TE) modes; on the other hand, Eq. (15) describes the modes whose magnetic field is in the plane of periodicity and they are called transversal magnetic (TM) modes. For the two configurations considered here ($\theta=0, \pi/2$), we observe comparing Eq. (15) with Eqs. (12) and (13) that the TM modes depend only on ϵ_e when $\theta=0$ and on ϵ_o when $\theta=\pi/2$ since they include the η_{zz} matrix only. On the other hand, when $\theta=0$ the TE modes depend on ϵ_o only; however, they depend on the orientation of the director in the plane xy when $\theta=\pi/2$. The TE modes for this case depend on ϵ_o , ϵ_e , and ϕ . For arbitrary orientations of the director in the plane xy , the nondiagonal elements of the dielectric tensor are different from zero and they must be included according to Eq. (14). Finally, it is not possible to obtain independent equations for the two independent modes if we propagate the EM waves out the plane of periodicity. In this case, the modes are coupled and the system of Eq. (7) must be solved completely. We have calculated the band structure for the square and triangular lattices. For the square lattice we considered the PC made of solid Si cylinders embedded in a LC matrix. From Eqs. (14) and (15), we observe that when the director is orientated along the axis of the cylinders, we obtain a set of equations similar to the isotropic case with the dielectric constant of the LC equal to ϵ_e and ϵ_o for the TE and TM modes, respectively. In Fig. 7, we show the band structure for this configuration using the same values for ϵ_e and ϵ_o as in the previous section. The radius of the Si cylinders is taken as $r=0.2a$. The empty circles correspond to the TE modes, whereas the solid circles correspond to the TM modes. From our calculations we observe that there is a small photonic band gap for the TM modes only at frequencies between 0.2819 and 0.2685. This is due to the contrast between the solid Si cylinders and the ϵ_e used in the equation for these modes. We calculated the band structure for the case when the director is perpendicular to the axis of the cylinders. In Fig. 8 we show the band structure for this configuration for two different orientations of the director \hat{n} in the plane of periodicity; $\phi=0$ and $\pi/2$. The solid circles correspond to the TM modes, whereas the open circles cor-

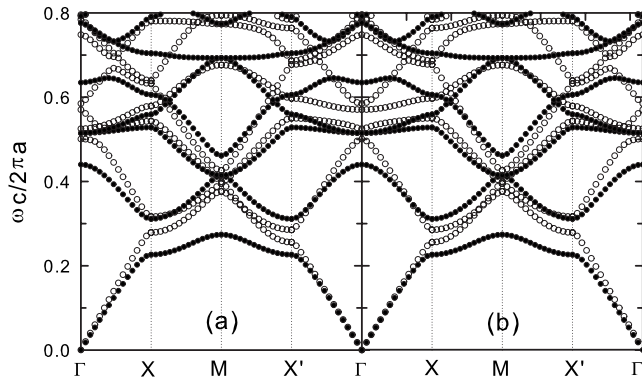


FIG. 8. Band structure for the square lattice of solid Si cylinders in a LC matrix with the director \hat{n} in the plane of periodicity ($\theta=\pi/2$). (a) $\phi=0$ and (b) $\phi=\pi/2$. Solid (empty) circles are for the TM (TE) modes.

respond to the TE modes. Figure 9(a) corresponds to the case $\phi=\pi/4$. From Figs. 8(a) and 8(b) we observe that the band structure for the TM modes is the same since according to Eqs. (13) and (15) the TM modes do not depend on the orientation of the director \hat{n} in the plane xy . Only the TE modes are dependent on the ϕ angle. We choose this system to compare our results with those reported in Ref. 6. Cheng-Yang *et al.* studied this system and they reported a ϕ -dependence on the band structure for the TM modes. Obviously their results are incorrect. From Fig. 1 of Ref. 6 we observe that for $\theta=\pi/2$ the TM modes have their corresponding electric field along the axis of the cylinders and therefore the equation, which describes these modes must contain ϵ_o only. This is the Eq. (15) of this paper, which depends only on ϵ_o according to Eq. (13). On the other hand, TE modes depend on ϕ because Eq. (14) includes the diagonal and nondiagonal elements of Eq. (13). We calculated the photonic band structure for all the values of the radius r corresponding to nonoverlapping Si cylinders in a LC matrix, for the conjugate lattice (LC cylinders in a Si matrix), and for different values of the angle ϕ . Unfortunately for this system there is no complete photonic band gap for the TE modes, which are the only modes that depend on the ϕ angle. From Figs. 8 and 9(a) we observe different irreducible Brillouin zones (IBZ) depending on the orientation of the direction \hat{n} of the LC background. This is because introducing

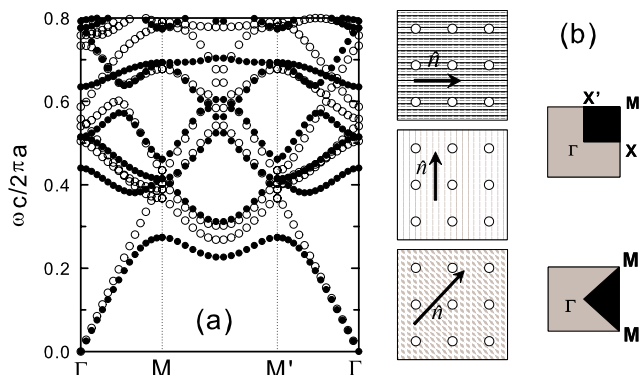


FIG. 9. (Color online) (a) Band structure for the TE (open circles) and TM (solid circles) with $\phi=\pi/4$. (b) Schematic representation for the orientation of the director \hat{n} in the plane of periodicity and correct IBZ used in the calculations.

anisotropic materials into the structure reduces the symmetry of the system. The correct IBZ is calculated by enumerating the point symmetry operations, which survive in the crystal after the infiltration of the LC. For the three cases considered in this work, only four symmetry operations survive from the eight symmetry operations of the C_{4v} .¹⁷ Of course the cases $\phi=0$ and $\phi=\pi/2$ are equivalent and they possess the same IBZ. Propagating an EM wave along the direction $\Gamma-X$ when $\phi=0$ will be equivalent to propagating along $\Gamma-X'$ when $\phi=\pi/2$. This equivalence can be observed by comparing the band structure along the $\Gamma-X$ direction of Fig. 8(a) with the band structure of Fig. 8(b) along the $\Gamma-X'$ direction. Of course, because the TM modes are independent of ϕ , the band structures displayed in Figs. 8 and 9(a) are all equivalent. This equivalence is clearly observed if we compare the band structure of half of the direction $M-M'$ of Fig. 9(a) with the band structure of Fig. 8(a) along the $M-X$ direction. In Fig. 9(b) we show schematically the orientations of the director and the different IBZs used for the calculations. From Fig. 8 we observe that the band structure along the $X-M$ and $M-X'$ directions seems symmetric with respect to inversion along the M point. Of course our crystal does not possess this symmetry. A careful analysis of the band structure confirms this statement; the frequencies obtained are different. In conclusion, the band structure for the EM waves propagating in the plane of periodicity of a square array of solid Si cylinders embedded in a LC anisotropic medium does not possess any complete photonic band gap for both polarizations. There is a complete photonic band gap for the TM modes only. However, these modes are independent of the orientation of the LC's director \hat{n} . Therefore, the photonic band gap of this system cannot be tuned by orientating the director \hat{n} .

However, it is well known that the triangular array of Si solid cylinders embedded in air possesses a complete photonic band gap for both polarizations.¹⁸ With the purpose to have a system with tunable photonic band gap, we have done calculations for a triangular array of LC cylinders embedded in a Si matrix. We considered LC cylinders with radius $r_0=0.48a$, a being the lattice constant and the values of ϵ_e and ϵ_o are the same as in the calculations for the square lattice discussed in the previous paragraph. In Fig. 10(a) we show the band structure for $\theta=0$ (director \hat{n} along the axis of the cylinders) and in Figs. 11(a)–11(c) we show the band structure with the director \hat{n} in the plane of periodicity ($\theta=\pi/2$) for $\phi=0$, $\phi=\pi/3$, and $\phi=\pi/2$, respectively. In all the figures, solid circles correspond to the TM modes and the open circles correspond to the TE modes. As we can see in the figures, for the values of dielectric constants used in this work, there is no complete photonic band gap for the TM modes. However, the TE modes exhibit a complete photonic band gap and the value of this gap can be tuned by an adequate orientation of the LC. As before, when the director \hat{n} is in the plane of periodicity, the band structure for the TM modes is independent of ϕ . Only the TE modes are dependent on the orientation of the LC since the equation describing these modes is dependent on the angle ϕ [see Eqs. (12)–(15)]. Again, we have different 2D IBZs depending on the orientation of \hat{n} in the plane $x-y$. For the cases consid-

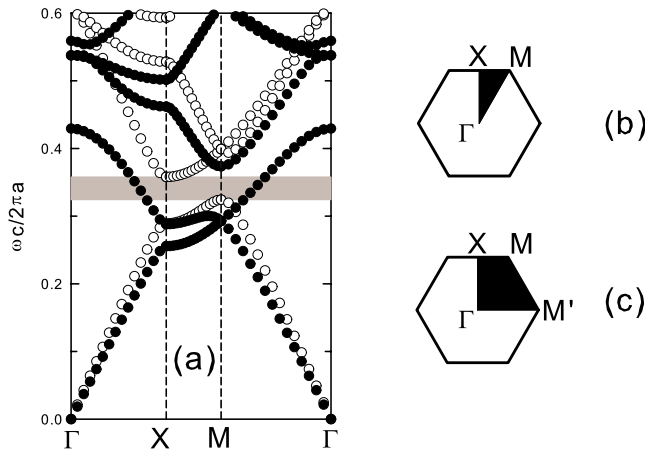


FIG. 10. (Color online) Band structure for the triangular lattice of LC cylinders embedded in a Si matrix. Solid (open) circles correspond to the TM (TE) modes. (a) Director \hat{n} along the axis of the cylinders ($\theta=0$). (b) IBZ for the director \hat{n} along the axis of the cylinders. (c) IBZ when \hat{n} is in the plane of periodicity for $\phi=0$, $\pi/2$ or $\phi=\pi/3$.

ered in this work, from the 12 symmetry operations of the group C_{3v} , only four symmetry operations survive after the infiltrations of LC cylinders. The correct IBZs for the different orientations of \hat{n} considered here are schematically shown in Figs. 10(b) and 10(c). Figure 10(b) is the IBZ for the case $\theta=0$ and this is the same for the isotropic case. Figure 10(c) is the IBZ for the case $\theta=\pi/2$ with $\phi=0$. Of course, the case $\theta=\pi/2$ with $\phi=0$, $\phi=\pi/3$, and $\phi=\pi/2$ has the same IBZ. In Figs. 10(b) and 10(c), the high symmetry points, along which the band structures of Figs. 10(a) and 11 were calculated, appear. From our results we can observe that only the TE modes are sensitive to the orientation of the director \hat{n} in the plane of periodicity. From our results we observe a shift in the band gap for the TE modes from $\omega a/2\pi c=0.3152-0.3216$ for $\phi=0$ to $0.3148-0.3484$ for $\phi=\pi/3$ and to $0.3148-0.3307$ for $\phi=\pi/2$.

V. CONCLUSIONS

We have calculated the photonic band structure for 1D and 2D PCs made by anisotropic LCs. Using the PW expansion

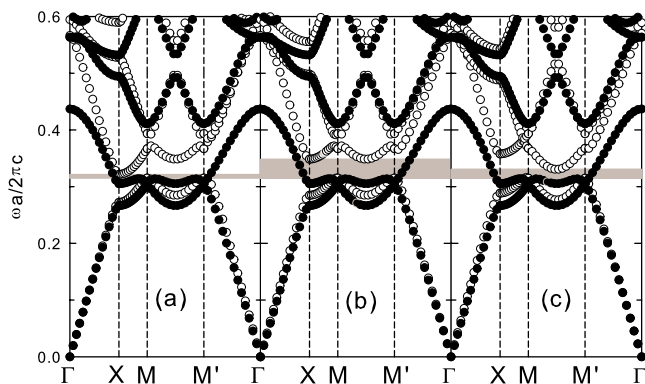


FIG. 11. (Color online) (a) The same as in Fig. 10 but $\theta=\pi/2$ and $\phi=0$. (b) and (c) correspond to $\phi=\pi/3$ and $\phi=\pi/2$, respectively.

sion to solve the Maxwell equations we have demonstrated that for the 1D case, it is possible to tune the photonic band gap by an adequate orientation of the director \hat{n} of the LC. This photonic band gap depends not only on the orientation of the director, but also on the direction of propagation of the EM wave. In the 2D case and for propagation in the plane of periodicity, we have shown that for the square array of solid Si cylinders in LC background it is not possible to tune the gap because only the TM modes present a complete photonic band gap and these modes are independent of the orientation of the LC's director \hat{n} . However, for the triangular array of LC cylinders surrounded by Si, this tune is possible for the TE modes only. For 2D PCs care must be taken in order to consider the correct IBZ. This IBZ is given by counting the number of symmetry operations, which survive after the infiltration of LC.

ACKNOWLEDGMENTS

One of the authors (J.A.) acknowledges the hospitality of the University of Lille, France, for the position as an invited professor offered to him during which this work was made. This work was supported by "Le fonds Européen de Développement Régional" (FEDER) INTERREG III France-Wallonie-Flanders (PREMIO) and "Le Conseil Régional Nord-Pas de Calais."

- ¹Z. Y. Li, B. Y. Gu, and G. Z. Yang, *Phys. Rev. Lett.* **81**, 2574 (1998).
- ²K. Busch and S. John, *Phys. Rev. Lett.* **83**, 967 (1999).
- ³D. Kang, J. E. MacLennan, N. A. Clark, A. A. Zakhidov, and R. H. Baughman, *Phys. Rev. Lett.* **86**, 4052 (2001).
- ⁴S. W. Leonard, J. P. Mondia, H. M. van Driel, S. Jhon, K. Bush, A. Birner, U. Gösele, and V. Lehman, *Phys. Rev. B* **61**, R2389 (2000).
- ⁵H. Takeda and K. Yoshino, *J. Appl. Phys.* **92**, 5658 (2002).
- ⁶C. Y. Liu and L. W. Chen, *Phys. Rev. B* **72**, 045133 (2005).
- ⁷G. Alagappan, X. W. Sun, P. Shum, M. B. Yu, and M. T. Doan, *J. Opt. Soc. Am. B* **23**, 159 (2006).
- ⁸G. Alagappan, X. W. Sun, P. Shum, and M. B. Yu, *J. Opt. Soc. Am. B* **23**, 1478 (2006).
- ⁹Ch. Schuller, J. P. Reithmaier, J. Zimmermann, M. Kamp, A. Forchel, and S. Anand, *Appl. Phys. Lett.* **87**, 121105 (2005).
- ¹⁰V. A. Tolmachev, T. S. Perova, S. A. Grudinkin, V. A. Melnikov, E. V. Astrova, and Yu. A. Zharova, *Appl. Phys. Lett.* **90**, 011908 (2007).
- ¹¹Q. Zhao, L. Kang, B. Du, B. Li, and J. Zhou, *Appl. Phys. Lett.* **90**, 011112 (2007).
- ¹²S. M. Weiss and P. M. Fauchet, *IEEE J. Sel. Top. Quantum Electron.* **12**, 1514 (2006).
- ¹³E. V. Astrova, T. S. Perova, Yu. A. Zharova, S. A. Grudinkin, V. A. Tolmachev, and V. A. Melnikov, *J. Lumin.* **121**, 298 (2006).
- ¹⁴J. Martz, R. Ferrini, F. Nüesch, L. Zuppiroli, B. Wild, L. A. Dunbar, R. Houdré, M. Mulot, and S. Anand, *J. Appl. Phys.* **99**, 103105 (2006).
- ¹⁵C. Y. Liu, Y. T. Feng, J. Z. Wang, and L. W. Chen, *Physica B* **388**, 124 (2007).
- ¹⁶K. M. Ho, C. T. Chan, and C. M. Soukoulis, *Phys. Rev. Lett.* **65**, 3152 (1990).
- ¹⁷G. Alagappan, X. W. Sun, P. Shum, M. B. Yu, and D. den Engelsen, *J. Opt. Soc. Am. A* **23**, 2002 (2006).
- ¹⁸J. D. Joannopoulos, R. D. Meade, and J. N. Winn, *Photonic Crystals: Molding the Flow of Light* (Princeton University Press, Princeton, NJ, 1995).